UDK 669.14.018.44:539.37
Original scientific article/Izvirni znanstveni članek

ISSN 1580-2949
MTAEC9, 47(6)819(2013)

STATIONARY-CREEP-RATE EQUATIONS FOR TEMPERED MARTENSITE

ENAČBE ZA HITROST STACIONARNEGA LEZENJA ŽARJENEGA MARTENZITA

Franc Vodopivec, Borut Žužek, Danijela A. Skobir Balantič, Monika Jenko, Matjaž Godec, Darja Steiner Petrovič

Institute of Metals and Technology, Lepi pot 11, 1000 Ljubljana, Slovenia
franc.vodopivec@imt.si

Prejem rokopisa – received: 2013-07-01; sprejem za objavo – accepted for publication: 2013-08-28

The stationary-creep equations including parameters as the average particle spacing or/and particle size are examined in terms of the effects of different equation parameters on the difference of calculated and experimental creep rate. It is concluded that the difference between the experimental creep rate and the creep rate deduced from the recently proposed creep equation is in the range of about ±25 % if the effects of the steel composition and the changes in the particle size and spacing during the creep test are considered with sufficient accuracy.

Keywords: creep-resistant steel, creep equations, particle size and spacing, difference between the calculated and experimental creep rate

Enačbe za izračun hitrosti stacionarnega lezenja, ki vključujejo kot parametre povprečno velikost in oddaljenost izločkov, so analizirane s stališča razlike med eksperimentalno in izračunano hitrostjo lezenja. Sklep je: pred kratkim predložena enačba da razliko v razponu okoli 25 %, če so prav upoštevani vplivi sestave jekla in spremembe velikosti in oddaljenosti izločkov pri preizkusih lezenja.

Ključne besede: jeklo odporno proti lezenju, enačbe za izračun hitrosti lezenja, velikost in oddaljenost izločkov, razlika med izračunano in eksperimentalno hitrostjo lezenja

1 INTRODUCTION

Theoretical and semi-empirical constitutive equations were proposed for calculating the stationary (secondary) creep rate of high-chromium creep-resistant steels using as parameters physical constants, creep-test conditions, steel properties, microstructure as well as the average particle size and spacing[1–5]. The equations were deduced applying different concepts of interaction between particle shape, size and spacing and mobile dislocations in the metal matrix. Also, more than 20 semi-empirical creep equations have been proposed[6–8] so far using the rationalisation of the stress-strain-creep test results obtained for different steels. In these equations, the base parameters of microstructures of creep-resistant steels, matrix grain size and particle size and spacing are considered as constants based on the results of the creep tests. The recently derived creep equation is based on the disjunctive-matrix (**dm**) concept of particle stress transfer of acting stress on gliding and climbing of dislocation segments in the matrix after crossing the strait between two neighbour particles[9]. By specific angles of acting stress, matrix grain-dislocation slip plane and stress-transfer particle face, the dislocation gliding stress is decreased significantly, while the climb stress changes much less[10]. It was concluded that the creep rate depended on the dislocation glide velocity in disjunctive matrix[9,10] which is proportional to the gliding stress[1]. The calculations have shown that in a disjunctive matrix with backstress due to opposite directions of the components of acting and transfer stress[10], the gliding stress may be decreased by up to about four orders of magnitude. The concept of a **dm** stationary creep of tempered martensite allows a simple explanation of the effect of matrix grain size on the stationary-creep rate and of the transition from stationary to accelerating creep[10]. In this article, the accuracy and reliability of parameters of the equations, proposed so far for calculating the stationary-creep rate, such as volume share, particle size and/or spacing are examined.

2 STATIONARY-CREEP EQUATIONS

Equation (1) was deduced for a dislocation line advancing through a field of obstacles (particles) by locally climbing over them[1]:

$$\dot{\varepsilon} = \left(\frac{2\pi \cdot D \cdot G \cdot b}{f \cdot k \cdot T}\right) \cdot \left(\frac{\sigma}{G}\right) \tag{1}$$

where $\dot{\varepsilon}$ is the creep rate (s^{-1}), D is the iron-diffusion rate in ferrite, G is the shear modulus at T, b is the Burgers vector, f is the volume fraction of particles in the matrix, k is the Boltzmann constant and σ is the acting stress.

It was stated that the equation is reasonable for the limit of density of mobile dislocations: $\rho < 1/(d/2)^2$. An

interaction of particles and mobile dislocations is considered including the volume share of carbide, *f*. In this work, experimental and calculated creep rates are obtained for the steel with the average particle sizes of d_1 = 280 nm and d_2 = 420 nm; the limits $\rho_1 = 1.96 \times 10^{14}$ m^{-2} and $\rho_2 = 4.41 \times 10^{14}$ m^{-2} are obtained, while $\rho = 0.978 \times 10^{14}$ m^{-2} is deduced later for the examined steel. Thus, the validity limit $\rho < 1/(d/2)^2$ for equation (1) is fulfilled.

Equation (2)[2] was derived as an improvement of equation (1) considering the density of mobile dislocations (ρ) and particle spacing (λ):

$$\dot{\varepsilon} = \frac{b^2 \cdot D \cdot \lambda \cdot \rho \cdot \sigma^2}{k \cdot T \cdot G} \tag{2}$$

For the detachment concept of stationary creep based on TEM observations of the detachment of the dislocation line from the free surface of oxide particles in aluminium, the creep equations (3) were derived[3–5]:

$$\dot{\varepsilon} = \left(\frac{6\lambda \cdot \rho \cdot D}{b}\right) \cdot \exp^{-E}$$

$$E = G \cdot b^2 \cdot r \cdot \left((1-k)\left[\frac{1-k}{\sigma_d}\right]\right)^{3/2} \tag{3}$$

where E is the detachment activation energy, σ_d is the detachment stress and $k = T_p/T_m$ with the T_m dislocation line energy.

It was concluded[11–13] that equations (3) required significant improvements for the calculation of the stationary-creep rate of the creep-resistant steels strengthened with non-coherent particles.

Equation (2) was modified introducing the constants for the particle size and spacing, considering their dependence on temperature and rationalising the acting stress with the shear modulus or yield stress at the creep-test temperature. Reasonable fits of the experimental and calculated creep rates for different test temperatures were obtained with the stress exponents in the range from n = 4.5 to n = 16 and the creep activation energy significantly higher than the activation energy of iron diffusion in ferrite was calculated[6–8,14–16]:

$$\dot{\varepsilon} = C_1 \cdot \left(\frac{\sigma}{G}\right)^n \cdot \exp^{-C_2 \frac{(\sigma/G)}{RT}} \tag{4}$$

Based on the experimental data[11–13], with $C_1 = 4.3 \times 10^{-41}$ K s^{-1} and $C_2 = 2.85 \times 10^7$, the stress exponent n = 4.5 and the activation energy of 680 kJ m^{-1} was deduced[16–18]. Recently, only a small difference was found in the creep activation energy for the creep rates calculated considering a negligible change in the particle size and spacing[19].

The simplified equation (5) includes the parameters of the previous equations and considers the effect of the particles as a difference of particle spacing and size ($\lambda - d$).[9] The basis of the equation is the assumption that the mobile-dislocation driving energy is consumed mainly for the lengthening of the dislocation segment due to the transition of the disjunctive-particle matrix. Based on the **dm** stationary-creep concept and experimental data, the stress exponent n = 3.65 was deduced and the obtained difference between the calculated and experimental creep rates was about 10 %.[9] For the cube-shaped particles, the exponent up to $n \approx 4$ was deduced recently[10]:

$$\dot{\varepsilon} = \frac{c \cdot b^2 \cdot \sigma^v \rho \cdot D \cdot (\lambda - d)}{k \cdot T \cdot G} \tag{5}$$

The creep rate ε in s^{-1} is obtained in equation (5) and written as:

$$\dot{\varepsilon} = c\alpha \frac{b^2 \cdot \sigma^v \rho \cdot D \cdot (\lambda - d)}{k \cdot T \cdot G} \text{ and } \alpha = \frac{\sigma^{3.65}}{\sigma^2} = 4.78 \cdot 10^3$$

The density of mobile dislocations was calculated as[18]:

$$\rho = \left(\frac{\sigma}{a \cdot M \cdot G \cdot b}\right)^2 \tag{6}$$

where M = 3 (the Taylor factor).

In **Table 1** for the tempered martensite with a uniform distribution of particles, the experimental creep rate, the creep rates calculated using equations (1), (2) and (5) with c = 1, $b = 2.5 \times 10^{-10}$ m, σ = 170 MPa, $\rho = 9.78 \times 10^{13}$ m^{-2}, $D = 1.19 \times 10^{-19}$ m^2 s^{-1} (in[19]), $k = 1.38 \times 10^{-23}$ J K^{-1}, $G = 57.3 \times 10^3$ MPa, T = 853 K and f = 0.037 (in[9,20]) are given.

Table 1: Creep rates calculated for two average particle sizes and spacings. In equation (1) shear stress $\sigma_g = \sigma_a/M$ = 170/3 = 56.6 GPa and in equation (5) n = 3.65 were considered.

Tabela 1: Hitrosti lezenja, izračunane za dve povprečni velikosti izločkov in razdalji med njimi. V enačbi (1) je upoštevan strižni modul $\sigma_g = \sigma_a/M$ = 170/3 = 56,6 GPa in n = 3,65.

Particles		Calc. creep rate, $\dot{\varepsilon}$/s^{-1}			Exp. creep rate
Size	Spacing	$\dot{\varepsilon}$			$\dot{\varepsilon}$
D	λ	s^{-1}			s^{-1}
nm	nm	Eq. 1	Eq. 2	Eq. 5	
280	1065	$2.36 \cdot 10^{-11}$	$3.42 \cdot 10^{-9}$	$12.2 \cdot 10^{-8}$	$12.1 \cdot 10^{-8}$
420	1650		$5.42 \cdot 10^{-9}$	$18.9 \cdot 10^{-8}$	$21.2 \cdot 10^{-8}$

The difference between the experimental and calculated creep rate for equation (5) is reasonable. It is greater if deduced from equation (1), probably due to the substitution of the effects of segmentation of the dislocation line, the interaction dislocation segments and the particles with the volume fraction of particles. The lower creep rate deduced from equation (4) is ascribed to the assumption of an interaction between the mobile dislocations and the modified Orowan mechanism. However, by stationary creep, the applied stress is significantly lower than the Orowan stress. The creep rates quoted in this work were determined and calculated for 100 h tests with static-tensile stress of 170 MPa at 853 K. At this temperature, the Young modulus (E) for two high-chromium creep-resistant steels is $E_{853} = 57.3 \times 10^3$ MPa

= 0.82 × E_{22} with the E_{22} Young modulus at room temperature[21]. Assuming that the effects of temperature on yield stress (σ_y) and Young modulus are equal, the experimental rates in **Table 2** were obtained as follows: $\sigma_{y853} \approx 0.82 \times \sigma_{y22} = 0.82 \times 400 = 328$ MPa. The ratio of the acting-creep stress to the yield stress, $\sigma/\sigma_y = 170/328 = 0.52$ at 853 K, makes the Orowan interaction between mobile dislocations and non-shearing particles improbable at the creep-test temperature.

3 ACCURACY AND RELIABILITY OF THE PARAMETERS IN EQUATION (5)

In creep-resistant steels, the ratio of numbers of iron atoms and atoms of the alloying elements is above 0.85. The difference between the parameters of chromium and iron is: Δ_a (Cr-Fe) = 2.88 × 10^{-10} – 2.48 × 10^{-10} = 0.4 × 10^{-10} m. Theoretically, the maximum extension of ferrite lattice due to chromium atoms in the solid solution is 0.4 × 0.15 = 0.06 × 10^{-10} m, thus 0.06/2.48 = 0.024 × 10^{-10} m. It is concluded that the effect of the difference in the Burgers vector due to alloying elements in solution in ferrite for creep-resistant steels is negligible.

The lattice parameters of ferrite and the Burgers vector are increased at the creep-test temperature because of the thermal expansion. The coefficient of linear thermal expansion of α iron is 11.8 × 10^{-6} K^{-1}. Consequently, at the creep-test temperature, the lattice parameter is for 2.48 × 10^{-10} × 11.6 × 10^{-6} × 853 = 2.45 × 10^{-12} m. Thus, the effect of increase in the α-Fe lattice at creep temperature is negligible.

The iron-diffusion rate was deduced from data in[19]. The values of activation energy for steels with 0.87 % Cr to 5 % Cr differ by less than 5 % from the average value. Considering the difference in D_0 it is concluded that the error due to differences in the diffusion rate is within ±10 %.

The acting stress is included as a parameter in all theoretical and semi-empirical equations, while $n = 1$, σ_a = 170 MPa, $\sigma^{1.1}$ = 284 MPa, $\sigma^{1.2}$ = 475 MPa, $\sigma^{1.5}$ = 2 116 MPa and σ^2 = 28 900 MPa. It is evident that already the difference of $n = 0.2$ generates the difference between the calculated and experimental creep rates of 2.8 times. The accuracy of the stress-exponent deduction depends on the accuracy of the assumed changes in particle content, size and spacing during the creep tests. The effect of the stress exponent is explained with the **dm** concept of the stationary creep[10]. It was, namely, calculated that the gliding stress in disjunctive parts of the matrix could be decreased by up to 10^4 times, with respect to the acting stress, to the backstress generated by the angles of acting stress, grain-dislocation slip plane and stress-transfer particle face. Thus, it seems reasonable to ascribe a great range of the quoted stress exponents (n = 4.5 to n = 16) to the undervaluation of the effect of changes of particle size and spacing during the experimental creep tests.

The mobile-dislocation density calculated using equation (5)[18], $\rho = 0.978 \times 10^{14}$ m^{-2}, was checked using the relations suggested for copper[22]:

$$\sigma_s = \frac{1}{2} \cdot G \cdot b \cdot \rho \quad \text{and} \quad \dot{\varepsilon} = \rho \cdot v \cdot b \tag{7}$$

where σ_s is the acting shear stress ($\sigma_s = \sigma_a/3$), v is the dislocation velocity, while the other parameters are the same as in equation (5); it was obtained that $\rho = 1.04 \times 10^{14}$ m^{-2}. The difference between the two deduced mobile-dislocation densities of 5.3 % supports the conclusion that the accuracy of the calculations of the mobile-dislocation density deduced from equation (6) is of ±10 %.

In the creep equations, the coefficient of iron diffusion in ferrite determined for the equilibrium content of vacancies is considered. The tensile stress increases the content of vacancies[23,24] and the increase in the diffusion rate is deduced from this relation[24]:

$$D_1 = \left(\frac{c_0}{c_1} \right) \cdot D_0 \tag{8}$$

where c_0 and D_0 are the vacancy content and diffusion rate at $\sigma = 0$, while c_1 and D_1 are the vacancy content and diffusion rate at the acting stress. It was deduced from data in[24] that $D_1 = 1.14D_0$. In the case of calculations of creep rate at the acting stress σ_a = 170 MPa, the effect of the increase of diffusion rate is relatively low with respect to the effect of the stress exponent, however, it should not be neglected in accurate calculations.

For the activation energy of iron diffusion in ferrite, $Q = \gamma$ and D_0 251 kJ/mol [19] as 289 kJ/mol [22] are quoted. The calculated diffusion rates at 853 K differ by several orders of magnitude. Thus, it is clear that the calculated creep-rate values are reliable only if deduced using reliable data in the deduction of iron diffusion in ferrite. In this case, the error in the calculation of the creep rates would be in the range of 10 %.

In modern high-chromium creep-resistant steels, the molar contents of carbide-forming vanadium and niobium are lower than the molar content of carbon, while the content of chromium is higher. Consequently, the particles of carbide $M_{23}C_6$ with a molar composition of $Cr_{18}Fe_3Mo_2$[23–25] are stable up to the austenite temperature. The solubility of VC and NbC carbides in ferrite is higher and at 700 °C virtually all VC and a significant part of NbC are dissolved in ferrite. Consequently, the effects of the creep-testing temperature on the quantity, size and spacing of particles of different carbides may be different. It is greater for a lower content of carbide-forming elements in solution in ferrite and higher solid solubility of carbide.

From the data in[25], it is calculated that in the 0.18C11.4Cr steel with the particles size of 0.1 μm, $M_{23}C_6$ increase after 1000 h at 650 °C by about Δd = 2 %, and by about Δd = 12 % at 750 °C. According to

equation (5), the creep rate is proportional to ($\lambda - d$). The particle spacing is deduced from[2]:

$$\lambda = \frac{4 \cdot d}{\pi \cdot f^{1/3}} \tag{9}$$

By constant volume share of carbide, an increase in average particle size of 12 %, the increase of particle spacing is $\Delta\lambda = 4\Delta d = 48$ % and, according to equation (5), the increase of difference between experimental and calculated creep rates of (48 – 12) % = 36 %. The logical conclusion is that by stationary-creep tests, reliable data could be obtained only by a very limited change initial particles size and spacing. The difference between calculated and experimental creep rates would be even greater if the dissolution of the VC and NbC particles was omitted.

Assuming that after the tempering at 800 °C $M_{23}C_6$ particles are situated in the centre of cubes with edge e, equation (10) was deduced[20]. Further, it was assumed that, in the micrograph plane, the sections of all cubes are squares with side e and with a particle in the square centre. The average size of the particle is than[20]:

$$d = \frac{\pi \cdot F^{1/2} \cdot f^{1/3}}{4N_{\mathrm{p}}^{1/2}} \tag{10}$$

where F is the surface area of the assessed micrograph and N_{p} is the number of the particles in the micrograph, f is the volume fraction of carbide calculated from the content of carbon in the steel and the previously quoted relation[2], $e = \lambda = (4d)/\pi\ f^{1/3}$. In equation (5) it is assumed that the cube edge and the square side lengths are equal. This assumption is partly incorrect, as the geometrical shape of a cube section depends on the angle between the section (micrograph) plane and the cube edge, which is, on average, a rectangle with the average side length $s = 1.205e = (e + e\sqrt{2})/2$[10]. The average spacing of the particles in the micrograph plane is then not $\lambda = \sqrt{F}/N$ but $\lambda' = 1.205\ \sqrt{F}/N$ and equation (10) is inexact. However, the size of most of the particles is below the average size[25]. On the SEM micrographs, the particles with the size of 25 nm are visible by magnification of 10^4 times. The dissolution velocity of particles, $v_{\mathrm{d}} \approx d^3/d^2$, is inversely proportional to the particle surface area[26]. As in equation (5) ($\lambda - d$) is included, it is assumed that the omission of the particles unseen on the micrographs at the magnification of 5×10^3 would decrease the calculated creep rate by up to 10 % if interaction particle-mobile dislocation was independent of particle size.

The volume fraction of carbide f is a parameter in several equations and it is deduced considering the contents of carbon and of carbide-forming elements in steel[2,20,27]. For high-chromium steels, the calculated value of f is accurate as the content of carbon is much higher than the content of chromium bound in $M_{23}C_6$. The calculation of the carbide-volume fraction is unreliable in case of a strong effect of temperature on the solubility of particles of different carbides, i.e., VC and NbC carbides in creep resistant steels. In this case, the volume fraction of carbides is calculated with an acceptable accuracy up to about 650 °C when vanadium in niobium are virtually totally bound in VC and NbC and the difference in carbon is bound to $M_{23}C_6$.

4 ACCURACY OF EQUATION (10)

Equation (10)[20] was deduced assuming:

- a spherical shape of the particles with different sizes,
- the particles are situated in the centres of the cubes of different sizes;
- the particle spacing is equal to the cube edge, which is equal to the square side on the micrographs and $\lambda = (F/N)^{1/2}$ with F – surface and N – number of particles on the examined micrograph.

In **Table 2** the results of an assessment of the micrographs of the same specimen of the X20 steel, quenched and tempered for 400 h at 800 °C, are listed. The volume fraction of carbide $Cr_{18}Fe_3Mo_2C_6$, with $f = 0.045$, in the steel tempered at 800 °C [20] was deduced as:

$$f = \frac{C \cdot \dfrac{(18Cr + 3Fe + 2Mo + 6C)}{6C}}{7.04 \times V_{\mathrm{st}}} \tag{11}$$

where C is the content of C in 100 g of steel in g; Cr, Fe, Mo and C are the atom weights; 7.04 is the specific weight of carbide (g/cm^3) and V_{st} is the volume of 100 g of steel.

Table 2: Results of assessment of micrographs of $M_{23}C_6$ particles in grip and gauge parts of a specimen after 100 h of creep tests with σ = 170 MPa and 853 K

Tabela 2: Rezultati analiz izločkov $M_{23}C_6$ na posnetkih iz merilnega in vpetega dela preizkušanca po preizkusu lezenja 100 h pri 853 K in 170 MPa

Magnification	Gauge, particles, μm		Grip, particles, μm	
	Spacing	Size	Spacing	Size
3500	0.68	0.19	0.72	0.20
5000	0.61	0.17	0.58	0.16
10000	0.55	0.15	0.55	0.15

The average particle spacing and size decrease with the micrograph magnification and reflect the discernibility of very small particles. By the magnification of 10^4 times, the particles of a size down to 25 nm are discerned. The omission of smaller particles would cause an error of about 10 % with respect to the particle spacing and size; however, this inaccuracy is diminished with the assumption that the section of the cubes in the micrograph plane is orthogonal to the cube edge, while the section is rectangular and the average particle spacing is, accordingly, greater. The resulting error is opposed to the error due to the number of very small particles undiscerned on the examined micrograph. The comparison of data suggests that by sufficient magnification of the micrographs and a sufficient number of counted parti-

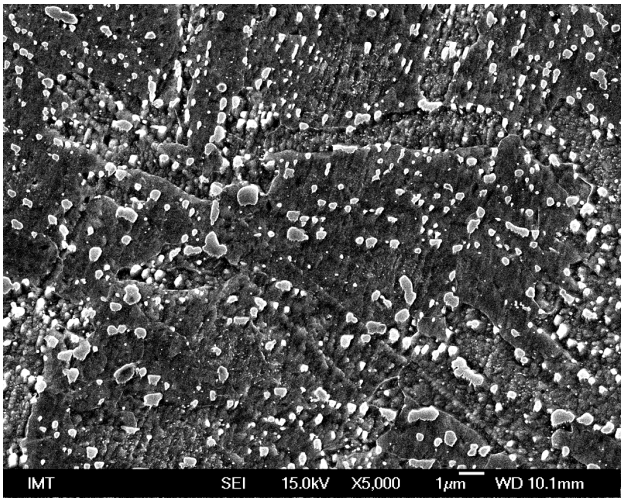

Figure 1: Particles in the gauge specimen part
Slika 1: Izločki v merilnem delu preizkušanca

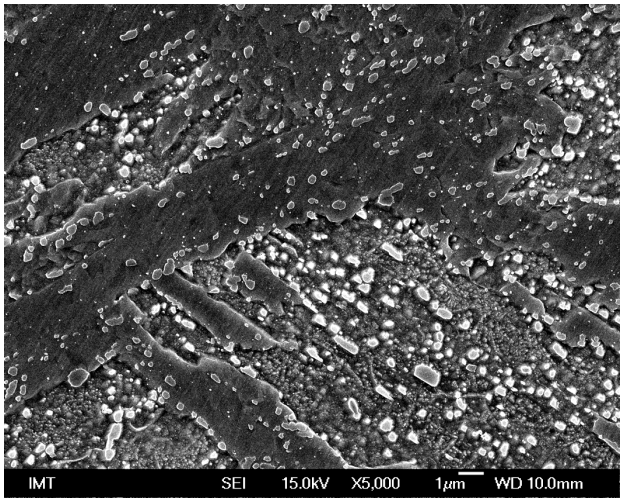

Figure 2: Particles in the grip specimen part with areas of inappropriate etching
Slika 2: Izločki v vpetem delu preizkušanca, ki ni bil pravilno jedkan

cles, the range of error of assessment the particle size and spacing is ±10 %.

The error could be significantly greater by insufficient surface quality of the SEM micrograph specimen. In **Figures 1** and **2** SEM micrographs of the same steel are shown. The surface quality of the specimen in **Figure 1** was sufficient and only $M_{23}C_6$ particles of different sizes are visible, while the quality of surface of the specimen in **Figure 2** was insufficient, as, in strongly etched areas, a great density of very small particles is visible due to an unsuited specimen preparation.

5 CONCLUSIONS

The accuracy of the quoted creep-rate equations, including as parameters particles size and spacing, depends on the accuracy of consideration of the changes due to the creep-test stress and temperature, and is related to:

- physical parameters at test temperature with a negligible change by change of test temperature;
- inaccuracies of the calculated changes in steel parameters: iron-diffusion rate in ferrite, shear modulus and mobile-dislocation density are in the range of ±10 %;
- changes of average particle-size spacing during the tests may be greater than 100 % depending on the creep-test temperature, time and solubility of particles in ferrite;
- accuracy and reliability of the stress exponent as, due to the exponent change of 0.2, the calculated creep rate increases 2.8 times.

Thus, if the effects of enumerated changes of parameters are considered with sufficient accuracy, especially the change in the particle size and spacing, the stress coefficient was deduced from tests enabling the acurate changes of particle size and spacing, the difference between the experimental creep rate and the rate calculated for tempered martensite using equation (5), should be in the range of ±25 %.

Acknowledgment

The authors thank the Slovenian Research Agency for the funding of this work.

6 REFERENCES

[1] M. F. Ashby, The mechanical effects of a dispersion of a second phase, Proc. of the 2nd Int. Conf. On Strength of Metals and Alloys, ASM, Metals Park, Ohio, 1970, 507–541
[2] E. Hornbogen, Einfluss von Teilchen einer zweiten Phase auf das Zeitverhalten, In: W. Dahl, W. Pitch, Festigkeits- und Bruchverhalten bei höheren Temperaturen, Verlag Stahleisen, Düsseldorf 1980, 31–52
[3] E. Artz, D. S. Wilkinson, Acta Metall., 34 (**1986**), 1893–1898
[4] E. Artz, J. Rösler, Acta Metall., 36 (**1988**), 1053–1060
[5] J. Rösler, E. Artz, Acta Metall., 36 (**1988**), 1043–1051
[6] K. H. Kloos, J. Granacher, M. Monses, Steel Res., 69 (**1998**), 446–453
[7] S. R. Holdsworth, Constitutive equations for creep curves and predicting service life, In: F. Abe, T. U. Kern, R. Wiswanathan, Creep resistant steels, Woodhead Publ. Lim., Cambridge, England 2008, 403–420
[8] B. Wilshire, H. Burt, Creep strain analysis for steel, In: F. Abe, T. U. Kern, R. Wiswanathan, Creep resistant steels, Woodhead Publ. Lim., Cambridge, England 2008, 421–445
[9] F. Vodopivec, B. Žužek, M. Jenko, D. A. Skobir Balantič, M. Godec, Mater. Sci. Tech., 29 (**2013**) 4, 451–455
[10] F. Vodopivec, F. Kafexhiu, B. Žužek, Stationary creep and glide stress for martensite with hypothetic cube particles, submitted to Mater. Sci. Tech.
[11] V. Sklenička, K. Kuharova, A. Dlouhy, J. Krejči, Materials for Advanced Power Engineering, part I, In: D. Coutsoradis (ed.), Kluver Academic Publishers, 1994, 435–444
[12] J. Čadek, V. Šustek, M. Pahutova, Mat. Sci. Eng. A, 225 (**1997**), 22–28

[13] J. Čadek, V. Šustek, High Temperature Materials and Processes, 16 (**1997**), 97–107
[14] A. Nagode, B. Ule, M. Jenko, L. Kosec, Steel Res. Int., 78 (**2007**), 638–642
[15] B. Ule, A. Nagode, Materials Sci. Techn., 23 (**2007**), 1367–1374
[16] B. Ule, A. Nagode, Scripta Mater., 57 (**2007**), 405–408
[17] B. Žužek, F. Vodopivec, B. Podgornik, M. Jenko, M. Godec, Mater. Tehnol., 46 (**2012**) 6, 661–664
[18] K. Maruyama, K. Sawada, J. Koike, ISIJ Intern., 41 (**2001**), 641–653
[19] H. Oikawa, Y. Iijima, Diffusion behaviour of creep-resistant steels, In: F. Abe, T. U. Kern, R. Wiswanathan, Creep resistant steels, Woodhead Publ. Lim., Cambridge, England 2008, 241–264
[20] F. Vodopivec, D. A. Skobir Balantič, M. Jenko, B. Žužek, M. Godec, Mater. Tehnol., 46 (**2012**) 6, 633–636
[21] Y. F. Yin, R. G. Faulkner, Physical and elastic behaviour of creep-resistant steels, In: F. Abe, T. U. Kern, R. Wiswanathan, Creep resistant steels, Woodhead Publ. Lim., Cambridge, England 2008, 217–240
[22] R. W. K. Honeycombe, The Plastic Deformation of Metals, 2nd ed., Edward Arnold, London 1985, 10–14
[23] I. V. Valikova, A. V. Nazarov, Simulation of Characteristics Determining Pressure Effects on Self Diffusion in BBC and FCC Metals, Physics of Metals and Metallography, 109 (**2010**), 220–226
[24] J. W. Jang, J. Kwon, B. J. Lee, Effect of stress on self-diffusion in bcc Fe. An atomistic simulation study, Scripta Mater., 63 (**2010**), 39–42
[25] F. Vodopivec, D. Steiner Petrovič, B. Žužek, M. Jenko, Coarsening rate of $M_{23}C_6$ particles in a high chromium creep resistant steel, Steel Res. Int., 84 (**2013**) 11, 1110–1114
[26] J. W. Martin, R. D. Doherty, B. Cantor, Stability of microstructure in metallic systems, 2nd ed., Cambridge Un. Press, 1997, 254
[27] D. A. Skobir, F. Vodopivec, M. Jenko, S. Spaić, B. Markoli, Z. Metallkd., 95 (**2004**) 11, 1020–1024